

Motion-R³: Fast and Accurate Motion Annotation via Representation-based Representativeness Ranking

Jubo Yu
Xiamen University

30920201153951@stu.xmu.edu.cn

Fengyi Fang
Xiamen University

34520182201469@stu.xmu.edu.cn

Zijiao Zeng
Tencent Technology
zijiaozeng@tencent.com

Tianxiang Ren
Xiamen University

30920201153939@stu.xmu.edu.cn

Kai Wang
Nanjing University Of Aeronautics and Astronautics

wk0806@nuaa.edu.cn

Yazhan Zhang
Tencent Technology
yazhanzhang@tencent.com

Shihui Guo
Xiamen University

guoshihui@xmu.edu.cn

Andreas Aristidou
University of Cyprus
a.m.aristidou@gmail.com

Yipeng Qin
Cardiff University
qiny16@cardiff.ac.uk

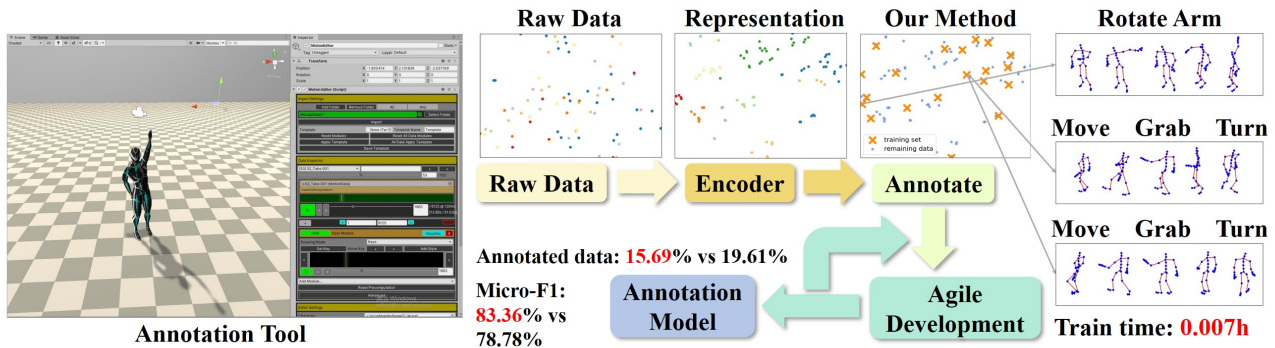


Figure 1. Overview of the proposed Motion-R³ method. Our method (bottom) i) reduces the time cost to (re)train motion annotation models by a factor of 500 to 700+, which allows for agile development; ii) achieves better micro-F1 scores with less manually annotated data, reducing the labour and time cost for manual annotation. Please see the *supplementary materials* for the demo of the proposed method.

Abstract

In this paper, we follow a data-centric philosophy and propose a novel motion annotation method based on the inherent representativeness of motion data in a given dataset. Specifically, we propose a Representation-based Representativeness Ranking (R³) method that ranks all motion data in a given dataset according to their representativeness in a learned motion representation space. We further propose a novel dual-level motion contrastive learning method to learn the motion representation space in a more informative way. Thanks to its high efficiency, our method is partic-

ularly responsive to frequent requirements change and enables agile development of motion annotation models. Experimental results on the HDM05 dataset against state-of-the-art methods demonstrate the superiority of our method.

1. Introduction

Along with the recent AI boom, data driven character animation has been revolutionized and dominated by deep learning [47, 48]. Despite its success, deep learning is known to be data-hungry, which poses challenges for

both academia and industry as high-quality annotated data are usually expensive and difficult to obtain. This is even more challenging for mocap (motion capture) data due to the large amount of data frames obtained from dense captures and the complex annotation procedure where multiple labels could be assigned to a single frame (i.e., an actor may wave while walking).

To minimize labour costs in annotation tasks, the best-performing methods resort to machine learning solutions. For example, Müller et al. [34] proposed to use motion templates and dynamic time warping (DTW) distance to segment and annotate motion data; Carrara et al. [8] proposed to use long short-term memory (LSTM) network to predict motion labels. Despite their differences, all these methods are *model-centric* and trained with expert-picked training data that are not suitable for machine use.

In this paper, we follow the *data-centric AI* philosophy advocated by Andrew Ng [36] and argue that the performance of motion annotation models can be significantly improved by simply using more representative samples in the training. Specifically, inspired by the classic farthest point sampling strategy, we propose a Representation-based Representativeness Ranking (R^3) method that ranks all motion data in a given dataset according to their “representativeness” in a learned motion representation space \mathcal{R} . To learn a more informative \mathcal{R} , we propose a novel dual-level contrastive learning method applied on both motion sequence and frame levels. In addition, the motion representation space \mathcal{R} learned by our method is independent to specific motion annotation tasks. This suggests that it is born to be adaptive to various motion annotation tasks, making it more responsive to frequent requirement changes and enabling agile development of motion annotation models. Experimental results on the HDM05 dataset against state-of-the-art methods demonstrate the superiority of our method. In summary, our main contributions include:

- We propose a novel motion annotation method (Motion- R^3) which significantly reduces the manual annotation workload without sacrificing the accuracy. Our method can rank motion data according to their “representativeness”. Results show that automatic motion annotation benefits significantly from the use of more representative training samples.
- We propose a novel dual-level motion contrastive learning method that can learn a more informative representation space for motion data.
- Our method only relies on the motion representations learned in an unsupervised way, which is more responsive to frequent requirement changes and enables agile development of motion annotation models.

2. Related Work

2.1. Motion Annotation

Motion annotation aims to annotate raw and unsegmented motion data with action labels, which is a complex and tedious task as multiple action labels can be assigned to the same piece of data [5, 65]. To address its challenges, a straightforward idea is to first divide the raw mocap data into action segments and then classify them respectively. For example, the sliding window method was employed to divide raw mocap data into overlapping action segments [32, 34, 56, 59] or non-overlapping semantic segments [6, 14, 38]. The classification of segmented action segments is usually referred to as an action recognition task, which aims to classify each action segment to the correct action category across different spatio-temporal configurations (e.g., velocity, temporal or spatial location) [4, 9, 16, 17, 25, 31, 37, 43, 46, 66]. Compared to traditional model-based methods [25, 54, 58] and classifiers [42, 52, 61], state-of-the-art action recognition methods resort to deep convolutional neural networks [26, 43] and LSTM neural networks [37, 45, 66] to effectively model spatial and temporal motion features, as deep learning has demonstrated its power in identifying complex patterns in multimedia data [2, 3]. On the other hand, frame-based motion annotation methods have recently gained popularity as they are more fine-grained and can predict the probabilities of each action per frame directly. The classification tasks in these methods are usually implemented by vector machines [44], linear classifiers [64], structured streaming skeletons [63], LSTM networks [8, 29, 46], etc. Furthermore, flow-based methods can identify motion before the motor behavior ends [28] and even predict future action [24, 55].

In this work, we investigate an important but underexplored problem in motion annotation, i.e., the representativeness of mocap data points. We demonstrate that the performance of motion annotation can be significantly improved by simply picking more representative samples for training (i.e., Representation-based Representativeness Ranking), which is orthogonal to all existing works.

2.2. Contrastive Learning

Contrastive learning is an unsupervised representation learning method that can learn high-quality feature spaces from unlabeled data [10, 12, 22, 50, 51, 57]. Contrastive Learning has made great progress in the field of computer vision [7, 10–13, 20–22, 50, 53, 57, 62]. And Momentum Contrastive Paradigm (MoCo) [12, 22] facilitates contrastive unsupervised learning through a queue-based dictionary lookup mechanism and momentum-based updates.

Contrastive learning has already been applied and achieved promising results in motion-related tasks. MS2L

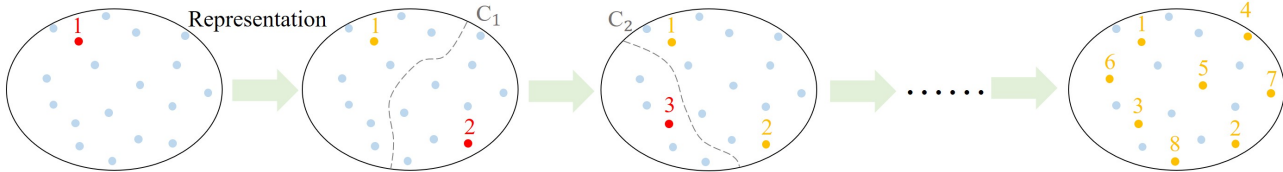


Figure 2. Illustration of our Representation-based Representativeness Ranking (R^3) method. **Blue**: motion sequences to be ranked. **Orange**: ranked motion sequences. **Red**: the next motion sequence in the ranking. C_n : a binary classifier.

[30] integrates contrastive learning into a multi-task learning framework; AS-CAL [41] uses different backbone sequence augmentations to generate positive and negative pairs; Thoker et al. [49] perform representation learning in a graph-based and sequence-based mode using two different network architectures in a cross-contrasted manner. Recently, SkeletonCLR [27] learns skeleton sequence representations through a momentum contrast framework. In a concurrent work, AimCLR [19] extends SkeletonCLR with an energy-based attention-guided casting module and nearest neighbor mining. BYOL [33] extends representation learning for skeleton sequence data and proposes a new data augmentation strategy, including two asymmetric transformation pipelines.

In this work, we propose a novel *dual-level* motion contrastive learning approach which extends MoCo [12, 22] to motion data and implements contrastive learning at both sequence and frame levels, which works as the basis of the proposed Motion- R^3 method.

2.3. Motion Represent

For example, Aristidou [1] employs comparative learning to generate high-dimensional motion features, which can be used in many applications for indexing, temporal segmentation, retrieval, and synthesis of motion clips. Bernard [5] operates a combination of hierarchical algorithms to create search groups and extract motion sequences. Zhou [65] applies alignment clustering analysis to action segmentation and expands standard kernel kmeans clustering through dynamic time warping (DTW) kernel to achieve temporary variance. Forbes [18] chooses weighted PCA to represent the pose, combined with the calculation of pose-to-pose distance, which is flexible and efficient, searching for similar motion sequences. Holden [23] utilizes an automatic convolutional encoder to learn a variety of human motion manifolds as a motion priori to resolve ambiguity.

3. Our Motion- R^3 Method

Let $D = (x_1, x_2, \dots, x_N)$ be a motion dataset consisting of N motion sequences, $x_i = (s_{i,1}, s_{i,2}, \dots, s_{i,T})$ be a motion sequence consisting of T consecutive skeleton pose frames, $s_{i,j} \in \mathbb{R}^{J \times 3}$ ($j = 1, 2, \dots, T$) be the 3D coordinates

of the J body joints of a skeleton pose, we aim to assign a binary label vector $\mathbf{c}_{i,j} = \{0, 1\}^m$ to each skeleton pose $s_{i,j}$ where $c_{i,j,k} = 1$ ($k = 1, 2, \dots, m$) if $s_{i,j}$ belongs to the k -th class of m pre-defined motion types. To minimize labour costs, we assume only a small portion of D are manually annotated as D_{train} and the rest can be automatically annotated by a machine learning model trained with D_{train} as the training set.

3.1. Overview

Unlike previous methods [8] which select D_{train} by visual inspection, we argue that picking the more *representative* ones for manual annotation not only reduces the labour and time costs but also increases the model’s accuracy. As Fig. 2 shows, our method aims to learn a representativeness ranking of motion sequences $x_i \in D$ in an unsupervised manner using the inherent similarities and differences among them by classifier C which consists of three linear layers. Alg. 1 shows the pseudo-code of our R^3 method.

Representation Learning We first train a feature encoder E which learns a representation space \mathcal{R} for x_i in an unsupervised manner. For the learning of feature encoder E and motion representation space \mathcal{R} , we adopt one of the latest contrastive learning approach: Momentum Contrast (MoCo) [12, 22], which has recently demonstrated superior performance and generalization abilities in computer vision tasks. Nevertheless, MoCo was designed for computer vision tasks and only works on the 2D grid-like image data. Thus, it is non-trivial to acclimatize it to motion sequences. Addressing this issue, we propose a *dual-level* motion contrastive learning approach which extends MoCo to motion data and implements contrastive learning at both sequence and frame levels, which is depicted in the next subsection.

Representativeness Ranking We next rank $x_i \in D$ according to their representativeness in \mathcal{R} . Inspired by the classic farthest point sampling strategy, we implement our R^3 method by progressively including $x_i \in D$ to a sorted motion dataset \hat{D} , where x_i is the “farthest” (*i.e.*, the most representative) motion sequence to the ranked ones in \hat{D} in the representation space \mathcal{R} . The ranking is then deter-

Algorithm 1: R³: Representation-based Representative Ranking

Data: Motion representation space \mathcal{R} , motion dataset $D = [x_1, x_2, \dots, x_T]$ and $\hat{D} = []$, binary classifier C .

Result: Sorted motion dataset \hat{D} .

- 1 $a \leftarrow$ a random number in $\{1, 2, \dots, T\}$;
- 2 $\hat{D} \leftarrow \hat{D}.append(x_a)$, $D \leftarrow D.remove(x_a)$;
- 3 **while** $D \neq []$ **do**
- 4 Train C to distinguish between elements of \hat{D} and D in \mathcal{R} ;
- 5 $x_a \leftarrow$ the most representative $x_i \in D$ according to C ;
- 6 $\hat{D} \leftarrow \hat{D}.append(x_a)$, $D \leftarrow D.remove(x_a)$;
- 7 **end**

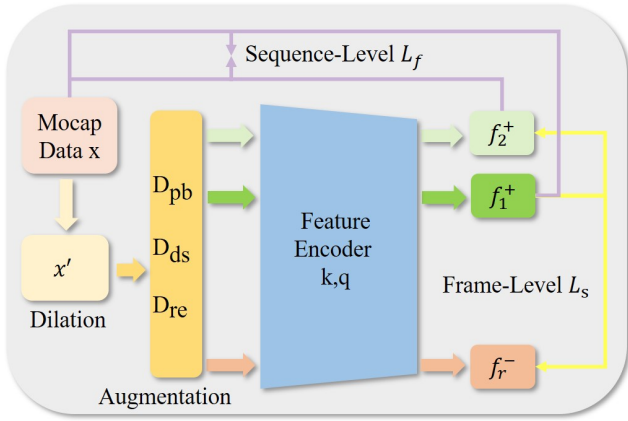


Figure 3. Dual-level Motion Contrastive Learning.

mined by the order in which x_i is included into \hat{D} . Note that we search the “farthest” points via binary classification to avoid the high computational costs of traditional farthest point sampling methods that consumes $O(n^2)$ time with decreasing to $O(n)$.

Motion Annotation with R³ For motion annotation, we first assign motion sequences to human annotators according to the ranking \hat{D} and get \hat{D}_{train} . Then, we train a low-cost and simple classifier C_{simple} using the learned representation \mathcal{R} and \hat{D}_{train} to annotate the remaining motion sequences automatically.

3.2. Dual-level Motion Contrastive Learning

In a nutshell, contrastive learning assumes that a good data representation has two properties: similar data points should be close to each other in the feature space, while different data points should be far from each other. Accordingly, it proposes to fulfil the two properties by minimiz-

ing the distances among positively augmented samples and maximizing those among negatively augmented samples. Building on this idea, MoCo [12, 22] shows that the performance of contrastive learning can be boosted by maintaining a large and consistent dictionary of negatively augmented samples, which is implemented by the incorporation of a queue and a momentum encoder. Thus, the extension of MoCo to *motion data* boils down to three questions: i) how to select a proper backbone network for feature encoding? ii) how to design the positive and negative data augmentation methods? iii) how to measure the distances between samples in the feature spaces (*i.e.*, the contrastive loss)?

3.2.1 Dilated (Momentum) Feature Encoder.

Since motion data are usually captured at a high sampling rate (*e.g.*, 120 FPS), the differences between adjacent frames are tiny, which causes ambiguities that confuse the model in identifying the action of a single frame. To clarify such ambiguity, we borrow the idea of *dilated* convolution [60] and enhance each input frame with its context information (*i.e.*, dilated joint trajectory) in a time window t centered at the current frame. Specifically, assuming the sampling rate is $r = 120$ FPS, we employ a dilation factor l that enhances input frame $s_{i,j}$ with its context information as

$$s'_{i,j} = (s_{i,j} - s_{i,j-nl}, \dots, s_{i,j} - s_{i,j-l}, s_{i,j}, s_{i,j+l} - s_{i,j}, \dots, s_{i,j+nl} - s_{i,j}) \quad (1)$$

where $n = \lfloor t \cdot r/l \rfloor$, $\lfloor \cdot \rfloor$ is a flooring function, $\pm(s_{i,j} - s_{i,j+kl})$ denotes the dilated joint trajectory, $k = \{-n, -n+1, \dots, n\}$. We use $x'_i = (s'_{i,1}, s'_{i,2}, \dots, s'_{i,T})$ as the input to our (momentum) feature encoders. We replace the Vision Transformer [15] with similar method as Spatial Temporal Transformer [39] as our feature encoder, for its success in modeling the dependencies among skeleton joints. Specifically, after being embedded in a two-layer MLP network, it models the relationships among joints of a single skeleton in each frame with the so-called Spatial Transformer (E_{ST}) module and those among the same joints across different frames in x'_i with its Temporal Self-Transformer (E_{TT}) module.

For the momentum feature encoder, we follow MoCo [12, 22] and update its parameters by:

$$\theta_k \leftarrow \alpha \theta_k + (1 - \alpha) \theta_q \quad (2)$$

where θ_k, θ_q denote the parameters of the momentum and native encoders, $\alpha \in [0, 1)$ denotes a momentum coefficient.

Since our motion data is a motion *sequence* consisting of consecutive *frames* of skeleton poses, we propose to implement contrastive learning at both levels as follows.

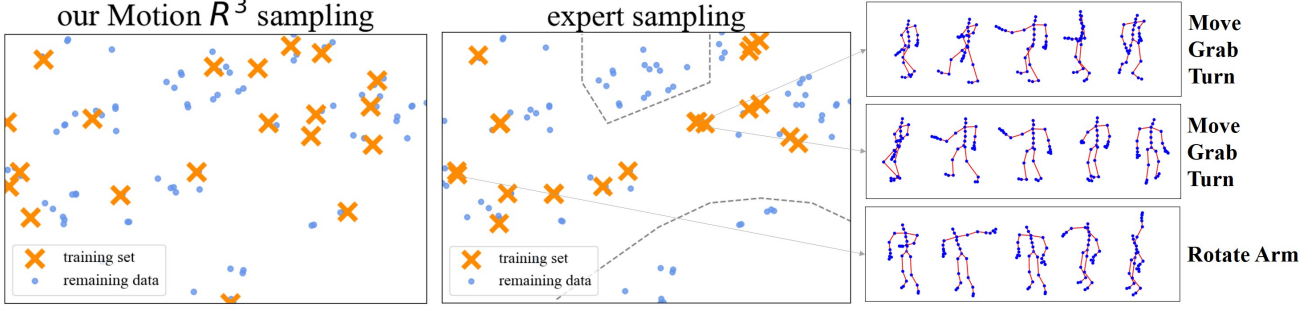


Figure 4. Comparison of sample representativeness of our Motion-R³ method against expert selection [8] in the feature space.

3.2.2 Sequence-Level Contrastive Learning

We show the data augmentation methods and loss design of the proposed sequence-level contrastive learning method below.

Sequence-level Data Augmentation. Similar to the applications of contrastive learning in computer vision tasks [10, 12, 22], the key challenge of motion data augmentation is to disentangle the inherent patterns of a skeleton from its different *views*, *i.e.*, the different appearances of the same pattern. Addressing this challenge, let $x' = (s'_1, s'_2, \dots, s'_T)$ be the enhanced input (Eq. 1),

i) We propose a *perturbation* data augmentation strategy with the rationale that motion semantics are robust against small perturbations. Specifically, we apply two stochastic perturbations, data missing and disorder, to each input frame s'_i according to $p_i \sim \mathcal{U}[0, 1]$ as follows:

$$pb(s'_i, p_i) = \begin{cases} 0, & p_i < t_{pb} \cdot t_{md} \\ s'_j, & t_{pb} \cdot t_{md} \leq p_i < t_{pb} \end{cases}, j \sim \mathcal{U}\{1, T\} \quad (3)$$

where $t_{pb} = 0.15 \in [0, 1]$ is the probability threshold that s'_i is perturbed, $t_{md} = 0.9 \in [0, 1]$ is the probability threshold that missing data perturbation is applied, $t_{pb} \cdot t_{md}$ means that s'_i is perturbed with missing data perturbation, the replacement of s'_i with s'_j denotes the disorder perturbation, $\mathcal{U}\{1, T\}$ denotes a discrete Uniform distribution from 1 to T . Let $p = p_i$, we have

$$\mathcal{D}_{pb}(x', p) = (pb(s'_1, p_1), pb(s'_2, p_2), \dots, pb(s'_T, p_T)) \quad (4)$$

ii) Inspired by the fact that human beings can successfully recognize motions at different playback speeds (*i.e.*, the motion semantics are largely independent of the playback speeds), we propose a novel *downsampling* data augmentation technique that creates novel views of motion data by downsampling them at random rates and offsets:

$$\mathcal{D}_{ds}(x', a, \delta) = (s'_a, s'_{a+\delta}, s'_{a+2\delta}, \dots, s'_{a+(n_{ds}-1)\delta}) \quad (5)$$

where a denotes the offset, δ denotes the downsampling interval, $n_{ds} = 512$ denotes the number of resulting samples. Note that $a + (n_{ds} - 1)\delta \leq T$.

iii) We also propose the *reverse* augmentation that works as a negative augmentation method:

$$\mathcal{D}_{re}(x') = (s'_T, s'_{T-1}, \dots, s'_1) \quad (6)$$

With the aforementioned data augmentation methods, we generate two positively augmented views v_1^+, v_2^+ and a negatively augmented view v_r^- as follows:

$$\begin{aligned} v_1^+ &= \mathcal{D}_{pb}(\mathcal{D}_{ds}(x', a^1, \delta^1), p^1) \\ v_2^+ &= \mathcal{D}_{pb}(\mathcal{D}_{ds}(x', a^2, \delta^2), p^2) \\ v_r^- &= \mathcal{D}_{re}(\mathcal{D}_{mk}(\mathcal{D}_{ds}(x', a^3, \delta^3), p^3)) \end{aligned} \quad (7)$$

where a^i, δ^i, p^i denote different parameters generated randomly.

We encode these augmented views and get their normalized features:

$$f_1^+ = \frac{E(v_1^+)}{\|E(v_1^+)\|}, f_2^+ = \frac{E(v_2^+)}{\|E(v_2^+)\|}, f_r^- = \frac{E(v_r^-)}{\|E(v_r^-)\|} \quad (8)$$

where E is the dilated (momentum) feature encoder.

Sequence-level Contrastive Loss. We design our loss function based on an InfoNCE loss:

$$\mathcal{L}_s = -\log \frac{\exp(f_1^+ \cdot f_2^+ / \tau)}{\exp(f_1^+ \cdot f_2^+ / \tau) + \sum_{i=1}^K \exp(f_1^+ \cdot f_i^- / \tau)} \quad (9)$$

where \cdot denotes the measurement of cosine similarity, τ is a temperature softening hyper-parameter and i denotes the indices of the negative samples f_i^- maintained in the queue Q of size K that

$$Q = f_r^- \frown \{f_1^-, f_2^-\} \quad (10)$$

where \frown denotes the enqueue operation, $\{f_1^-, f_2^-\}$ denotes the positive samples generated previously but are used as negative samples for f_1^+ as they are generated from different x' .

3.2.3 Frame-level Contrastive Learning

Frame-level Data Augmentation. Leveraging the *local consistency* among consecutive frames in a motion sequence (i.e., the actions in a small neighbourhood share similar motion semantics), for the feature $f_{1,i}^+$ of each frame s'_i , we define $f_{2,j}^+$ are its *positive* samples if $j \in \Omega_+$ and $\Omega_+ = \{j | t_{nb} > |i - j|\}$, where $t_{nb} = 12$ is the size of the neighbourhood, and vice versa ($f_{2,j}^-$ is *negative* if $j \in \Omega_-$ and $\Omega_- = \{j | t_{nb} \leq |i - j|\}$).

Frame-level Contrastive Loss. Accordingly, we design our frame-level local consistency loss as:

$$\mathcal{L}_f = -\log \sum_i \sum_{j \in \Omega_+} \exp(f_{1,i}^+ \cdot f_{2,j}^+ / \tau) \quad (11)$$

3.2.4 Overall Loss Function

Combining the sequence-level loss \mathcal{L}_s and the frame-level loss \mathcal{L}_f , we have:

$$\mathcal{L} = \mathcal{L}_s + \omega \mathcal{L}_f \quad (12)$$

where $\omega = 1$ is a weighting parameter.

4. Experiments & Results

4.1. Implementation Details

We conduct experiments on a PC with an Intel i7-7700 CPU and a Nvidia TESLA P40 GPU. We implement our method with PyTorch. We follow the method of Sedmidubsky J [43] to process motion data, and normalize the position, orientation and Skeleton size. Following [8], we evaluate our method on the three variants of the HDM05 dataset [35]:

- **HDM05-15:** 102 motion sequences in 15 classes, consuming 68 minutes and 491,847 frames;
- **HDM05-65:** 2,345 motion sequences in 65 classes, consuming 156 minutes and 1,125,652 frames;
- **HDM05-122:** 2,238 motion sequences in 122 classes, consuming 156 minutes and 1,125,652 frames.

Note that HDM05-65 and HDM05-122 contain the same data but have different labels.

BABEL [40] is a large-scale human motion dataset with rich motion semantics labeling, annotating motion capture data from AMASS for about 43.5 hours. We used the 22-joint skeleton position from SMPL-H in AMASS and combined BABEL to annotate actions in the motion sequence. BABEL has two versions, consisting of 60 and 120 action category tags. We performed experiments in both cases. And we use micro-F1 as our main evaluation metric.

4.2. Motion Representativeness

As Fig. 4 shows, the samples selected by our Motion-R³ method is more evenly distributed according to the entire data distribution and are more representative than those selected by the expert [8], which justifies the effectiveness of our Motion-R³ method.

The top right corner of expert sampling (in the middle part of Fig. 4) shows the four pairs of samples are close to overlapping. A visual inspection shows that they are highly similar, i.e., one pair shows the same move-grab-turn activity. In contrast, there are vast unlabeled samples, which are highlighted as two bounded regions. The samples in these two regions largely fall into the categories of exercise and move-turn, which are significantly different from other labeled ones. The quantitative results show that the prediction accuracy of these neglected categories are below average.

It is also worth pointing out that the evaluation and ranking of motion representativeness are fully automatic. However, the expert needs to investigate all data before annotation, in order to select suitable samples for the training set. The selection is highly dependent on the skill and experience of the expert. Suitable samples require appropriate data distribution covering all action classes.

4.3. Comparison with State-of-the-Art



Figure 5. Annotation result of comparison with [8] against annotated data on HDM05-15 dataset.

To demonstrate the superiority of our Motion-R³ method, we quantitatively compare it with two state-of-the-

Table 1. Comparison with state-of-the-art motion annotation methods: Müller [34] and Carrara [8] on the HDM05-15, HDM05-65 and HDM05-122 datasets. “Train” and “Test” show the data split percentages of the dataset. Ours¹: the minimum amount of data required by our method to achieve higher accuracy than “Expert + Carrara”, *i.e.*, [8]. Ours²: the accuracy of our method when using the same amount of training data as “Expert + Carrara”, *i.e.*, [8]. \mathcal{R} +MLP: train a simple Multi-layer perceptron using the learned motion representation space \mathcal{R} . Müller*: we did not test “Ours^{1,2} + Müller” as the source code of [34] was not publicly released.

Method		HDM05-15		HDM05-65		HDM05-122	
Sampling	Annotation	Train (%)	micro-F1 (%)	Train (%)	micro-F1 (%)	Train (%)	micro-F1 (%)
Expert	Müller*	28.57	75.00	-	-	-	-
Expert	Carrara	19.61	78.78	44.12	64.82	44.12	57.66
Ours ¹	Carrara	<u>15.69</u>	79.20	40.76	65.00	42.02	58.42
Ours ²	Carrara	19.61	80.50	44.12	67.00	44.12	60.70
Ours ¹	\mathcal{R} +MLP	15.69	79.05	<u>25.21</u>	65.56	<u>22.68</u>	59.94
Ours ²	\mathcal{R} +MLP	19.61	<u>83.66</u>	44.12	<u>71.13</u>	44.12	<u>68.69</u>

art motion annotation methods [8, 34] on the HDM05-15, HDM05-65 and HDM05-122 datasets. The resulting annotations are shown in Fig. 5. Ours can be closer to Ground Truth than Carrara [8].

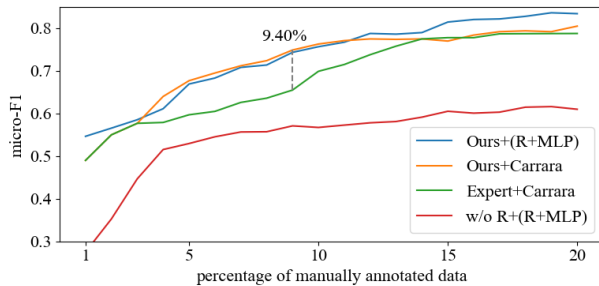


Figure 6. Comparison with [8] against percentage of manually annotated data on HDM05-15 dataset. Ours+Carrara significantly outperforms the vanilla Expert+Carrara (*e.g.*, by 9.40%) when using 3%-12% manually annotated data.

As Fig. 6 shows, training [8] with the representative samples provided by our Motion-R³ method (Ours+Carrara) helps the model to reach its performance saturation point much faster than its vanilla version trained with expert-selected training data (Expert+Carrara), which indicates a better trade-off between accuracy and speed/amount of manual annotation for our method. To further demonstrate the power of our data-centric method, we show that the performance of our method using a simple MLP (Multi-layer Perceptron) predictor trained on the learned motion representation space \mathcal{R} (Ours+ \mathcal{R} +MLP) can achieve slightly better performance than [8] (Expert+Carrara). Note that it only takes about 5 seconds to train our MLP predictor, which allows for agile development of motion annotation models (Sec. 5).

Table 1 shows the experimental results of the minimum amount of data required by our methods (Ours+Carrara and Ours+ \mathcal{R} +MLP) to achieve higher accuracy than [8] (Expert+Carrara) and the accuracy of our method when using the same amount of training data as [8]. Surprisingly, we observed that Ours+ \mathcal{R} +MLP outperforms Ours+Carrara for HDM05-65 and HDM05-122 datasets, which further demonstrates the power of our data-centric method and the learned motion representation. Note that the “illusion” of less improvement stems from the fact that the amount of data used by [8] is far more than is required to reach performance saturation and our method still significantly outperforms it when using less data.

4.4. Experiment on BABEL

We also tested our Motion-R³ in BABEL [40]. We divide train, test and val dataset according to BABEL. We pre-trained our model on the train dataset and tested our method on the val dataset.

Table 2. Results on BABEL [40]: We report our Motion-R³ on both BABEL60 and BABEL120.

Train (%)	BABEL60 (%)	BABEL120 (%)
5	19.59	16.91
10	20.00	17.16
20	21.45	21.77
30	22.83	24.09
40	25.74	24.42
50	25.93	24.74

4.5. Robustness Against Initial Selection

Since the performance of our method selects the initial element (*i.e.*, the element with the highest “representative-

Table 3. Robustness of our method against random choices of the initial element.

Training (%)	1	5	10	20
micro-F1(%)	33.7±19.9	61.0±6.5	72.3±2.8	81.8±1.8

ness”) randomly, we examine the robustness of our method with its statistics over multiple runs with different initial elements.

Table 3 shows our experimental results. The performance variance is large (18.9%) when the training data is only 1%. In this case, the selection of the initial element is critical. It can be observed that the performance deviations quickly converge to a small number, i.e., the variance reduces to 1.7% when the training data comes to 20%. This indicates that the selection of initial element does not affect the performance of our method. This justifies the robustness of our method.

4.6. Ablation Study

4.6.1 Design of Dual-level contrastive Learning

As Table 4 shows, the experimental results justify the effectiveness of the algorithmic designs of our dual-level contrastive learning method.

Table 4. Ablation Study on the Algorithmic Designs of our Dual-level Contrastive Learning. MoCo baseline*: naive adaptation of MoCo [22] to our task.

Method	micro-F1(%)	macro-F1(%)
MoCo baseline*	59.31	39.54
<i>Sequence Level</i>		
+perturbation	59.75	56.98
+diluted encoder	63.44	56.28
+downsampling	81.21	76.49
+reverse	82.07	77.09
<i>Frame Level</i>		
+local consistency	83.66	77.55

The results show that the contrastive learning on both the sequence and frame levels contributes to the final performance. The four designs on the sequence level play a more important role in boosting the performance of our method, compared with the one on the frame level. The results with the native Moco method show that it is not directly applicable to the task of motion annotation.

4.6.2 Performance without Motion Representation

We justify the effectiveness of the motion representation learned by our Dual-level Contrastive Learning by compar-

ing it with a variant of our representativeness ranking algorithm applied directly to the raw motion data.

As Fig. 6 shows, it can be observed that our method consistently outperforms its raw data variant. With the increasing number of annotated data, the gap between the conditions of using and without using motion representation enlarges. When the number of annotated data is 5%, the accuracy difference is 2.6%; while the number of annotated data is 20%, this metric increases to 6.7%.

5. Application in Agile Development

Due to the subjective nature of annotation and the inherent ambiguity in motion labels, a motion annotation model should be responsive to frequent requirement change to be applied in industry. Unlike previous methods [8] that train prediction models in an end-to-end manner, our method splits the learning into two stages: i) a motion representation learning stage that is independent to annotation and ii) a light-weight MLP predictor training stage, and is thus born to be adaptive to frequent requirement changes. Specifically, the motion representations learned by our method are *reusable* and the MLP predictor that requires retraining takes only about 5 seconds to train for a single run.

To demonstrate the superiority of our method against frequent requirement changes, we design a prototype toolkit of motion annotation using Unity3D, as visualized at the beginning of this paper. The toolkit can insert keyframes at the beginning and end of the action to label, train the classifier and predict annotation for the rest samples in the dataset. To verify the effectiveness of our toolkit, a set of dummy test cases assumes that the required numbers and types of classes and manual annotation frequently changes from HDM05-15 to HDM05-65, and finally to the HDM05-122 dataset. The subscript of t_{15} , t_{65} , t_{122} denotes the corresponding dataset.

As Table 5 shows, our algorithm runs approximately 500 to 700+ times faster than [8] while achieving better micro-F1 scores (Table 1), under the condition of frequent requirement changes. This effectively shows the advantage of our method. This efficiency and flexibility guarantees its advantage in practical applications in real world.

Table 5. Comparison with Carrara [8] on agile development. t_{pre} : time cost of pre-training; $t_n(h)$: time cost of retraining a model to satisfy the requirement of the HDM05- n dataset. We use hour (h) as the time unit.

method	t_{pre}	t_{15}	t_{65}	t_{122}
Carrara	-	3.5	7.3	10.1
Our	1.3	0.007	0.012	0.013

6. Limitation

We found that in HDM05-15 dataset, it is often difficult to accurately identify the action types with ambiguous semantics, such as "neutral", whose separate F1 score is only 57%, while the F1 score of other actions is about 70 -90%.

7. Conclusion

In this paper, we propose a novel motion annotation method, namely Motion-R³, which shows that the performance of motion annotation can be significantly improved by using the more representative training samples extracted by our Representation-based Representativeness Ranking (R³) method. Our R³ method relies on an informative representation space learned by the proposed novel dual-level motion contrastive learning method. Thanks to its high efficiency, our Motion-R³ method is particularly responsive to frequent requirement changes and enables agile development of motion annotation models, which sheds light on a new working paradigm for both the academia and the industry.

Our future work aims to: 1) explore the full potential of our method in larger dataset, by using other sources of motion data, such as 3D pose estimation of computer vision; 2) further improve the accuracy of the model and reduce the requirement of annotated data size, e.g., by improving the contrastive learning model.

References

- [1] Andreas Aristidou, Daniel Cohen-Or, Jessica K. Hodgins, Yiorgos Chrysanthou, and Ariel Shamir. Deep motifs and motion signatures. *ACM Trans. Graph.*, 37(6), dec 2018. 3
- [2] Maryam Asadi-Aghbolaghi, Albert Clapes, Marco Bellantonio, Hugo Jair Escalante, Víctor Ponce-López, Xavier Baró, Isabelle Guyon, Shohreh Kasaei, and Sergio Escalera. A survey on deep learning based approaches for action and gesture recognition in image sequences. In *2017 12th IEEE international conference on automatic face & gesture recognition (FG 2017)*, pages 476–483. IEEE, 2017. 2
- [3] Tadas Baltrušaitis, Chaitanya Ahuja, and Louis-Philippe Morency. Multimodal machine learning: A survey and taxonomy. *IEEE transactions on pattern analysis and machine intelligence*, 41(2):423–443, 2018. 2
- [4] Mathieu Barnachon, Saïda Bouakaz, Boubakeur Boufama, and Erwan Guillou. Ongoing human action recognition with motion capture. *Pattern Recognition*, 47(1):238–247, 2014. 2
- [5] Jürgen Bernard, Nils Wilhelm, Björn Krüger, Thorsten May, Tobias Schreck, and Jörn Kohlhammer. Motionexplorer: Exploratory search in human motion capture data based on hierarchical aggregation. *IEEE transactions on visualization and computer graphics*, 19(12):2257–2266, 2013. 2, 3
- [6] Said Yacine Boulahia, Eric Anquetil, Franck Multon, and Richard Kulpa. Cudi3d: Curvilinear displacement based approach for online 3d action detection. *Computer vision and image understanding*, 174:57–69, 2018. 2
- [7] Mathilde Caron, Ishan Misra, Julien Mairal, Priya Goyal, Piotr Bojanowski, and Armand Joulin. Unsupervised learning of visual features by contrasting cluster assignments. *Advances in Neural Information Processing Systems*, 33:9912–9924, 2020. 2
- [8] Fabio Carrara, Petr Elias, Jan Sedmidubsky, and Pavel Zezula. Lstm-based real-time action detection and prediction in human motion streams. *Multimedia Tools and Applications*, 78(19):27309–27331, 2019. 2, 3, 5, 6, 7, 8
- [9] Chen Chen, Roozbeh Jafari, and Nasser Kehtarnavaz. A survey of depth and inertial sensor fusion for human action recognition. *Multimedia Tools and Applications*, 76(3):4405–4425, 2017. 2
- [10] Ting Chen, Simon Kornblith, Mohammad Norouzi, and Geoffrey Hinton. A simple framework for contrastive learning of visual representations. In *International conference on machine learning*, pages 1597–1607. PMLR, 2020. 2, 5
- [11] Ting Chen, Simon Kornblith, Kevin Swersky, Mohammad Norouzi, and Geoffrey E Hinton. Big self-supervised models are strong semi-supervised learners. *Advances in neural information processing systems*, 33:22243–22255, 2020. 2
- [12] Xinlei Chen, Haoqi Fan, Ross Girshick, and Kaiming He. Improved baselines with momentum contrastive learning. *arXiv preprint arXiv:2003.04297*, 2020. 2, 3, 4, 5
- [13] Xinlei Chen and Kaiming He. Exploring simple siamese representation learning. In *Proceedings of the IEEE/CVF Conference on Computer Vision and Pattern Recognition*, pages 15750–15758, 2021. 2
- [14] Maxime Devanne, Stefano Berretti, Pietro Pala, Hazem Wanous, Mohamed Daoudi, and Alberto Del Bimbo. Motion segment decomposition of rgb-d sequences for human behavior understanding. *Pattern Recognition*, 61:222–233, 2017. 2
- [15] Alexey Dosovitskiy, Lucas Beyer, Alexander Kolesnikov, Dirk Weissenborn, Xiaohua Zhai, Thomas Unterthiner, Mostafa Dehghani, Matthias Minderer, Georg Heigold, Sylvain Gelly, et al. An image is worth 16x16 words: Transformers for image recognition at scale. *arXiv preprint arXiv:2010.11929*, 2020. 4
- [16] Yong Du, Wei Wang, and Liang Wang. Hierarchical recurrent neural network for skeleton based action recognition. In *Proceedings of the IEEE conference on computer vision and pattern recognition*, pages 1110–1118, 2015. 2
- [17] Georgios Evangelidis, Gurkirt Singh, and Radu Horaud. Skeletal quads: Human action recognition using joint quadruples. In *2014 22nd International Conference on Pattern Recognition*, pages 4513–4518. IEEE, 2014. 2
- [18] Kate Forbes and Eugene Fiume. An efficient search algorithm for motion data using weighted pca. In *Proceedings of the 2005 ACM SIGGRAPH/Eurographics symposium on Computer animation*, pages 67–76, 2005. 3
- [19] Tianyu Guo, Hong Liu, Zhan Chen, Mengyuan Liu, Tao Wang, and Runwei Ding. Contrastive learning from extremely augmented skeleton sequences for self-supervised action recognition. *arXiv preprint arXiv:2112.03590*, 2021. 3

- [20] Michael Gutmann and Aapo Hyvärinen. Noise-contrastive estimation: A new estimation principle for unnormalized statistical models. In *Proceedings of the thirteenth international conference on artificial intelligence and statistics*, pages 297–304. JMLR Workshop and Conference Proceedings, 2010. 2
- [21] Raia Hadsell, Sumit Chopra, and Yann LeCun. Dimensionality reduction by learning an invariant mapping. In *2006 IEEE Computer Society Conference on Computer Vision and Pattern Recognition (CVPR'06)*, volume 2, pages 1735–1742. IEEE, 2006. 2
- [22] Kaiming He, Haoqi Fan, Yuxin Wu, Saining Xie, and Ross Girshick. Momentum contrast for unsupervised visual representation learning. In *Proceedings of the IEEE/CVF conference on computer vision and pattern recognition*, pages 9729–9738, 2020. 2, 3, 4, 5, 8
- [23] Daniel Holden, Jun Saito, Taku Komura, and Thomas Joyce. Learning motion manifolds with convolutional autoencoders. In *SIGGRAPH Asia 2015 technical briefs*, pages 1–4, 2015. 3
- [24] Ashesh Jain, Amir R Zamir, Silvio Savarese, and Ashutosh Saxena. Structural-rnn: Deep learning on spatio-temporal graphs. In *Proceedings of the IEEE conference on computer vision and pattern recognition*, pages 5308–5317, 2016. 2
- [25] Harshad Kadu and C-C Jay Kuo. Automatic human mocap data classification. *IEEE Transactions on Multimedia*, 16(8):2191–2202, 2014. 2
- [26] Sohaib Laraba, Mohammed Brahimi, Joëlle Tilmanne, and Thierry Dutoit. 3d skeleton-based action recognition by representing motion capture sequences as 2d-rgb images. *Computer Animation and Virtual Worlds*, 28(3-4):e1782, 2017. 2
- [27] Linguo Li, Minsi Wang, Bingbing Ni, Hang Wang, Jiancheng Yang, and Wenjun Zhang. 3d human action representation learning via cross-view consistency pursuit. In *Proceedings of the IEEE/CVF Conference on Computer Vision and Pattern Recognition*, pages 4741–4750, 2021. 3
- [28] Sheng Li, Kang Li, and Yun Fu. Early recognition of 3d human actions. *ACM Transactions on Multimedia Computing, Communications, and Applications (TOMM)*, 14(1s):1–21, 2018. 2
- [29] Yanghao Li, Cuiling Lan, Junliang Xing, Wenjun Zeng, Chunfeng Yuan, and Jiaying Liu. Online human action detection using joint classification-regression recurrent neural networks. In *European conference on computer vision*, pages 203–220. Springer, 2016. 2
- [30] Lilang Lin, Sijie Song, Wenhan Yang, and Jiaying Liu. Ms2l: Multi-task self-supervised learning for skeleton based action recognition. In *Proceedings of the 28th ACM International Conference on Multimedia*, pages 2490–2498, 2020. 3
- [31] Jun Liu, Gang Wang, Ling-Yu Duan, Kamila Abdiyeva, and Alex C Kot. Skeleton-based human action recognition with global context-aware attention lstm networks. *IEEE Transactions on Image Processing*, 27(4):1586–1599, 2017. 2
- [32] Moustafa Meshry, Mohamed E Hussein, and Marwan Torki. Linear-time online action detection from 3d skeletal data using bags of gesturelets. In *2016 IEEE Winter Conference on Applications of Computer Vision (WACV)*, pages 1–9. IEEE, 2016. 2
- [33] Olivier Moliner, Sangxia Huang, and Kalle Åström. Bootstrapped representation learning for skeleton-based action recognition. *arXiv preprint arXiv:2202.02232*, 2022. 3
- [34] Meinard Müller, Andreas Baak, and Hans-Peter Seidel. Efficient and robust annotation of motion capture data. In *Proceedings of the 2009 ACM SIGGRAPH/Eurographics Symposium on Computer Animation*, pages 17–26, 2009. 2, 7
- [35] Meinard Müller, Tido Röder, Michael Clausen, Bernhard Eberhardt, Björn Krüger, and Andreas Weber. Documentation mocap database hdm05. 2007. 6
- [36] Andrew Ng. Unbiggen ai. *IEEE Spectrum.*, 2022. 2
- [37] Juan C Nunez, Raul Cabido, Juan J Pantrigo, Antonio S Montemayor, and Jose F Velez. Convolutional neural networks and long short-term memory for skeleton-based human activity and hand gesture recognition. *Pattern Recognition*, 76:80–94, 2018. 2
- [38] Konstantinos Papadopoulos, Enjie Ghorbel, Renato Baptista, Djamilia Aouada, and Björn Ottersten. Two-stage rgb-based action detection using augmented 3d poses. In *International Conference on Computer Analysis of Images and Patterns*, pages 26–35. Springer, 2019. 2
- [39] Chiara Plizzari, Marco Cannici, and Matteo Matteucci. Spatial temporal transformer network for skeleton-based action recognition. In *International Conference on Pattern Recognition*, pages 694–701. Springer, 2021. 4
- [40] Abhinanda R Punnakkal, Arjun Chandrasekaran, Nikos Athanasiou, Alejandra Quiros-Ramirez, and Michael J Black. Babel: Bodies, action and behavior with english labels. In *Proceedings of the IEEE/CVF Conference on Computer Vision and Pattern Recognition*, pages 722–731, 2021. 6, 7
- [41] Haocong Rao, Shihao Xu, Xiping Hu, Jun Cheng, and Bin Hu. Augmented skeleton based contrastive action learning with momentum lstm for unsupervised action recognition. *Information Sciences*, 569:90–109, 2021. 3
- [42] Michalis Raptis, Darko Kirovski, and Hugues Hoppe. Real-time classification of dance gestures from skeleton animation. In *Proceedings of the 2011 ACM SIGGRAPH/Eurographics symposium on computer animation*, pages 147–156, 2011. 2
- [43] Jan Sedmidubsky, Petr Elias, and Pavel Zezula. Effective and efficient similarity searching in motion capture data. *Multimedia Tools and Applications*, 77(10):12073–12094, 2018. 2, 6
- [44] Amr Sharaf, Marwan Torki, Mohamed E Hussein, and Motaz El-Saban. Real-time multi-scale action detection from 3d skeleton data. In *2015 IEEE Winter Conference on Applications of Computer Vision*, pages 998–1005. IEEE, 2015. 2
- [45] Deepika Singh, Erinc Merdivan, Ismini Psychoula, Johannes Kropf, Sten Hanke, Matthieu Geist, and Andreas Holzinger. Human activity recognition using recurrent neural networks. In *International cross-domain conference for machine learning and knowledge extraction*, pages 267–274. Springer, 2017. 2
- [46] Sijie Song, Cuiling Lan, Junliang Xing, Wenjun Zeng, and Jiaying Liu. Spatio-temporal attention-based lstm networks

- for 3d action recognition and detection. *IEEE Transactions on image processing*, 27(7):3459–3471, 2018. 2
- [47] Sebastian Starke, Yiwei Zhao, Taku Komura, and Kazi Zaman. Local motion phases for learning multi-contact character movements. *ACM Transactions on Graphics (TOG)*, 39(4):54–1, 2020. 1
- [48] Sebastian Starke, Yiwei Zhao, Fabio Zinno, and Taku Komura. Neural animation layering for synthesizing martial arts movements. *ACM Transactions on Graphics (TOG)*, 40(4):1–16, 2021. 1
- [49] Fida Mohammad Thoker, Hazel Doughty, and Cees GM Snoek. Skeleton-contrastive 3d action representation learning. In *Proceedings of the 29th ACM International Conference on Multimedia*, pages 1655–1663, 2021. 3
- [50] Yonglong Tian, Dilip Krishnan, and Phillip Isola. Contrastive multiview coding. In *European conference on computer vision*, pages 776–794. Springer, 2020. 2
- [51] Aaron Van den Oord, Yazhe Li, and Oriol Vinyals. Representation learning with contrastive predictive coding. *arXiv e-prints*, pages arXiv–1807, 2018. 2
- [52] Antonio W Vieira, Thomas Lewiner, William Robson Schwartz, and Mario Campos. Distance matrices as invariant features for classifying mocap data. In *Proceedings of the 21st International Conference on Pattern Recognition (ICPR2012)*, pages 2934–2937. IEEE, 2012. 2
- [53] Pascal Vincent, Hugo Larochelle, Yoshua Bengio, and Pierre-Antoine Manzagol. Extracting and composing robust features with denoising autoencoders. In *Proceedings of the 25th international conference on Machine learning*, pages 1096–1103, 2008. 2
- [54] Chunyu Wang, Yizhou Wang, and Alan L Yuille. An approach to pose-based action recognition. In *Proceedings of the IEEE conference on computer vision and pattern recognition*, pages 915–922, 2013. 2
- [55] Chenxia Wu, Jiemi Zhang, Silvio Savarese, and Ashutosh Saxena. Watch-n-patch: Unsupervised understanding of actions and relations. In *Proceedings of the IEEE conference on computer vision and pattern recognition*, pages 4362–4370, 2015. 2
- [56] Huimin Wu, Jie Shao, Xing Xu, Yanli Ji, Fumin Shen, and Heng Tao Shen. Recognition and detection of two-person interactive actions using automatically selected skeleton features. *IEEE Transactions on Human-Machine Systems*, 48(3):304–310, 2017. 2
- [57] Zhirong Wu, Yuanjun Xiong, Stella X Yu, and Dahua Lin. Unsupervised feature learning via non-parametric instance discrimination. In *Proceedings of the IEEE conference on computer vision and pattern recognition*, pages 3733–3742, 2018. 2
- [58] Lu Xia, Chia-Chih Chen, and Jake K Aggarwal. View invariant human action recognition using histograms of 3d joints. In *2012 IEEE computer society conference on computer vision and pattern recognition workshops*, pages 20–27. IEEE, 2012. 2
- [59] Yan Xu, Zhengyang Shen, Xin Zhang, Yifan Gao, Shujian Deng, Yipei Wang, Yubo Fan, I Eric, and Chao Chang. Learning multi-level features for sensor-based human action recognition. *Pervasive and Mobile Computing*, 40:324–338, 2017. 2
- [60] Fisher Yu and Vladlen Koltun. Multi-scale context aggregation by dilated convolutions. In Yoshua Bengio and Yann LeCun, editors, *4th International Conference on Learning Representations, ICLR 2016, San Juan, Puerto Rico, May 2-4, 2016, Conference Track Proceedings*, 2016. 4
- [61] Mihai Zanfir, Marius Leordeanu, and Cristian Sminchisescu. The moving pose: An efficient 3d kinematics descriptor for low-latency action recognition and detection. In *Proceedings of the IEEE international conference on computer vision*, pages 2752–2759, 2013. 2
- [62] Richard Zhang, Phillip Isola, and Alexei A Efros. Colorful image colorization. In *European conference on computer vision*, pages 649–666. Springer, 2016. 2
- [63] Xin Zhao, Xue Li, Chaoyi Pang, Quan Z Sheng, Sen Wang, and Mao Ye. Structured streaming skeleton—a new feature for online human gesture recognition. *ACM Transactions on Multimedia Computing, Communications, and Applications (TOMM)*, 11(1s):1–18, 2014. 2
- [64] Xin Zhao, Xue Li, Chaoyi Pang, Xiaofeng Zhu, and Quan Z Sheng. Online human gesture recognition from motion data streams. In *Proceedings of the 21st ACM international conference on Multimedia*, pages 23–32, 2013. 2
- [65] Feng Zhou, Fernando De la Torre, and Jessica K Hodgins. Hierarchical aligned cluster analysis for temporal clustering of human motion. *IEEE Transactions on Pattern Analysis and Machine Intelligence*, 35(3):582–596, 2012. 2, 3
- [66] Wentao Zhu, Cuiling Lan, Junliang Xing, Wenjun Zeng, Yanghao Li, Li Shen, and Xiaohui Xie. Co-occurrence feature learning for skeleton based action recognition using regularized deep lstm networks. In *Proceedings of the AAAI conference on artificial intelligence*, volume 30, 2016. 2